OPEN ACCESS
IOP Publishing
Journal of Optics
J. Opt. **24** (2022) 045502 (9pp)
https://doi.org/10.1088/2040-8986/ac5289

The role of asymmetry in few-cycle, mid-IR pulses during THz pulse generation

Roland Flender[1], **Adam Borzsonyi**[1,2] **and Viktor Chikan**[1,3,*]

[1] ELI-ALPS, ELI-HU Non-Profit Ltd, Wolfgang Sandner utca 3, H-6728 Szeged, Hungary
[2] Department of Optics and Quantum Electronics, University of Szeged, Dóm tér 9, H-6720 Szeged, Hungary
[3] Department of Chemistry, Kansas State University, 213 CBC Building, Manhattan, KS 66506-0401, United States of America

E-mail: viktor.chikan@eli-alps.hu and vchikan@ksu.edu

Received 7 January 2022
Accepted for publication 7 February 2022
Published 22 February 2022

Abstract

The efficiency of terahertz (THz) pulse generation improves at longer driving wavelengths. For this reason, the use of mid-infrared (MIR) sources is more advantageous compared to visible or near-infrared systems. In this work, we investigate how single-color and two-color schemes of MIR pulses with few-cycle pulse durations compare in producing THz pulses. The results reveal that as the duration of the driving pulses decreases, the second harmonic generation crystal can be omitted from the system. Our numerical study pinpointed three regions where the optimal pulse parameters are fundamentally different for the most efficient THz pulse generation. The first is the two-color approach, where the two-color scheme is dominant at 3.2 optical cycles and over. The second is the single-color approach, where the single-color scheme becomes dominant at 1.7 optical cycles and below. Therefore, it simplifies the traditional two-color scheme for THz pulse generation. There is also a third transitional region where the two-color scheme still prevails, but the sign of the relative phase between the input pulses becomes important. Considering the effect of the relative phase and the carrier to envelope phase (CEP) effect on the THz pulse generation, the results have shown that as the pulse duration become shorter, the role of the CEP becomes important for efficient THz generation. By measuring the efficiency of the THz generation in this optical arrangement, quantifying the CEP becomes possible, which could become an important experimental tool for few-cycle, MIR laser technology.

Keywords: terahertz pulse, mid-infrared pulse, carrier to envelope phase, two-color pulses, few-cycle pulses

(Some figures may appear in color only in the online journal)

* Author to whom any correspondence should be addressed.

1. Introduction

One of the recent trends in scientific laser technology is to develop few-cycle, mid-infrared (MIR) laser sources [1–6]. Compared to visible and near-infrared sources, longer carrier wavelengths are preferable for secondary source development, which based on the ionization or acceleration of charged particles. The underlying physical phenomenon is that the ponderomotive potential scales with the square of the carrier wavelength of the driving laser pulse, which results in a higher cut-off for high harmonic generation (HHG) [7] and more intense terahertz (THz) pulse generation [8–15]. Additionally, these secondary sources also benefit from the few-cycle pulse durations and the control over the carrier to envelope phase (CEP) [1–6]. From the technical standpoint, these few-cycle, MIR lasers can also operate at high repetition rates, which is mainly due to the available pump lasers. The high repetition rates of these laser sources support HHG and THz generation by significantly reducing data accumulation times for these low-yield processes [16].

Recent studies have demonstrated that the intensity of THz pulse generation greatly improves with increasing carrier wavelength of the driving laser pulses [8–15]. These works are based on the so-called two-color scheme, where the fundamental and its second harmonic laser pulses simultaneously ionize and accelerate the free electrons in a gas medium. As mentioned earlier, one of the key reasons for more intense THz pulse generation is the role of the ponderomotive potential that scales with the square of the carrier wavelength. Another important benefit of the longer wavelength of the MIR laser pulses is the smaller differences between the group and phase velocities of the two-color pulses [9, 11, 12]. The small difference between the group velocities ensures better temporal overlap between the pulses. The challenge at these wavelengths is to control the relative phase between the pulses due to small differences between phase velocities. However, there are existing solutions in the literature to address this issue [15, 17]. First, THz pulse generation is highly sensitive to the asymmetry of the external electric field, which is associated with the relative phase of the two-color pulses. When the relative phase is $\pm\pi/2$ rad, the acceleration of the free electrons becomes the least symmetric and a significant, nonvanishing electron current builds up inside the plasma [18, 19], which is the source of the THz radiation. Second, the asymmetry of the external electric field is also associated with the number of optical cycles in the pulse. As the number of optical cycles decreases, the potential to produce more asymmetry in the electric field increases. The generation of sub-three-cycle laser pulses is still demanding, but numerous studies have already demonstrated its feasibility [20–25]. The few-cycle pulse duration requires hundreds of nm spectral bandwidth in the MIR spectral region, which is not easy to produce, and the management of the spectral phase is also complicated. The two-color scheme for THz pulse generation is less cumbersome due to the use of renewable sources such as air. However, the use of few-cycle laser pulses as a driving source for THz pulse generation further simplifies the construction of a THz source. Such a secondary source eliminates the need for nonlinear crystals for second harmonic generation (SHG) and for the use of thin plates for relative phase control. The absence of these optical elements in the beam path reduces reflection and conversion losses and eliminates the dispersion.

In this present work, we aim to investigate THz pulse generation with few-cycle, MIR laser pulses and compare the single-color and two-color schemes. The contribution of various processes to THz pulse generation is carefully considered for both schemes. The results indicate that there are three important regions where the optimal laser pulse parameters are fundamentally different for the generation of the most intense THz pulses. We also investigate the carrier wavelength dependence of the boundaries between these newly identified regions. Furthermore, we also investigated the relative phase and the CEP effect on the THz pulse generation.

2. Numerical model

The full description of our numerical model was already presented in our previous study [15]. Therefore, here we only briefly summarize the main steps with the necessary equations, which are based on the transient photocurrent model [18, 19]. Here, the driving pulses build up a transverse electron current inside the plasma, which radiates an electromagnetic wave with an angular frequency inversely proportional to the duration of the driving laser pulse [18, 19]. The schematic flow chart of our numerical model is shown in figure 1.

In brief, our simulation uses the method of slowly varying amplitude approximation [26] to calculate the second harmonic (SH):

$$\frac{\mathrm{d}A_1}{\mathrm{d}z} = \frac{2id_{\mathrm{eff}}\omega_1^2}{k_1c^2}A_2A_1^*\mathrm{e}^{-i\Delta kz} \text{ and} \tag{1}$$

$$\frac{\mathrm{d}A_2}{\mathrm{d}z} = \frac{id_{\mathrm{eff}}\omega_2^2}{k_2c^2}A_1^2\mathrm{e}^{i\Delta kz} \tag{2}$$

where A_1 (A_2) is the fundamental (SH) wave amplitude, d_{eff} is half of the effective value of the nonlinear susceptibility, ω_1 (ω_2) is angular frequency of the fundamental (SH) beam, k_1 (k_2) is the wavenumber of the fundamental (SH) beam and finally c is the speed of light. In our research, Z-cut gallium–selenide (GaSe) selected as a nonlinear medium. Its refractive index [27] and its effective nonlinear coefficient ($d_{22} = 86$ pm V^{-1}) [28] are well known in the corresponding literature. The d_{eff} can be calculated by $d_{22} \times \cos(\theta)$, where θ is the phase matching angle, which can be calculated by $2 \times k_1 = k_2(\theta)$ for type I phase matching (ooe). In this case the fundamental pulse is ordinary (o) polarized, while the SH pulse is extraordinary (eo) polarized. After solving the equations (1) and (2) numerically for a small propagation (Δz), the dispersion of both waves can be calculated by the following:

$$A_1(z+\Delta z) = A_1(z)\,\mathrm{e}^{-i2\pi n_1\Delta z/\lambda_1}, \tag{3}$$

$$A_2(z+\Delta z) = A_2(z)\,\mathrm{e}^{-i2\pi n_2\Delta z/\lambda_2}, \tag{4}$$

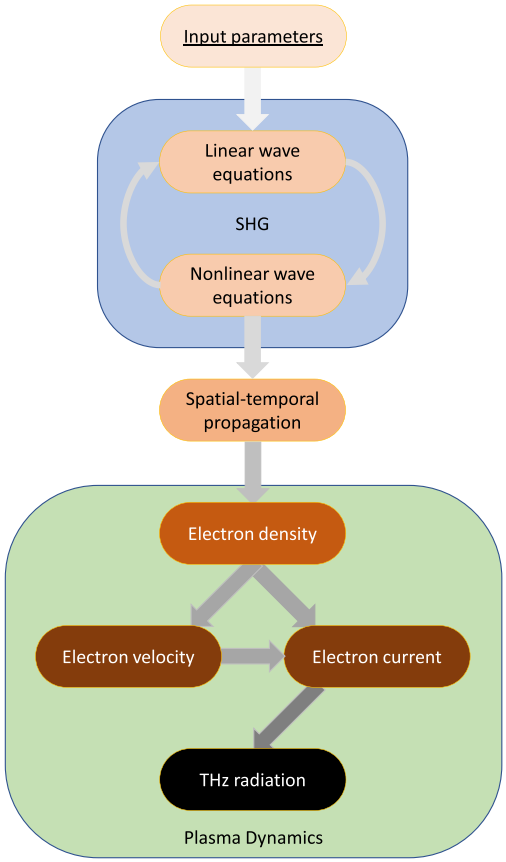

Figure 1. Schematic flow chart of the steps of our numerical model.

where λ_1 (λ_2) is the fundamental (SH) wavelength and n_1 (n_2) is the refractive index of the GaSe at the fundamental (SH) wavelength. The complex amplitude was calculated at each wavelength, while taking the GaSe's dispersion into account. These two steps were repeated through the whole thickness of the nonlinear crystal. The reflection loss on both surfaces, the dispersion and the temporal walk-off between the pulses are also considered.

In the following step, the focusing of the beams is calculated based on the ABCD law [29]. In the focus, the field ionization rate (W) is calculated based on the Ammosov–Delone–Krainov formula [30, 31]:

$$W = 1.61\omega_{\mathrm{au}}\frac{Z^2}{n_{\mathrm{eff}}}\left(10.87\frac{Z^2}{n_{\mathrm{eff}}^4}\frac{E_{\mathrm{au}}}{E}\right)^{2n_{\mathrm{eff}}^{-1.5}}\mathrm{e}^{\left(-\frac{2}{3}\frac{Z^3}{n_{\mathrm{eff}}^3}\frac{E_{\mathrm{au}}}{E}\right)}, \quad (5)$$

where ω_{au} is the atomic unit of frequency (4.1×10^{16} s^{-1}) and E_{au} is the atomic unit of field (5.14×10^9 Vcm^{-1}). E is the combined electric field, Z is the residual charge seen by the free electrons. The effective quantum number (n_{eff}) is defined by the following:

$$n_{\mathrm{eff}} = Z\Big/\sqrt{I_{\mathrm{n}}/I_{\mathrm{H}}}, \quad (6)$$

where I_{H} is the ionization potential of hydrogen (13.6 eV) and I_{N} is the ionization potential of nitrogen (15.58 eV) [31]. The second and higher order ionizations can be neglected in our case due to the moderate intensity used during the numerical simulations. The electron density (n_{e}) can be calculated using equation (5) and the rate equations, which are defined as the following:

$$n_{\mathrm{e}} = N_1, \quad (7)$$

$$\frac{\mathrm{d}N_0}{\mathrm{d}t} = -W_1 N_0 \text{ and} \quad (8)$$

$$\frac{\mathrm{d}N_1}{\mathrm{d}t} = +W_1 N_0, \quad (9)$$

where N_0 is the density of the unionized nitrogen, N_1 is the density of the singly ionized nitrogen. Once the electrons are free at $t = t'$, they are accelerated by the external electric field. The time varying velocity of the electrons can be calculated by the following:

$$v(t,t') = -\frac{e}{m_{\mathrm{e}}}\int_{t'}^{t} E(t)\,\mathrm{d}t, \quad (10)$$

where e is the charge of a single electron (1.60×10^{-19} C) and m_{e} is the mass of a single electron (9.11×10^{-31} kg). The free electrons not only oscillate in the external electric field, but also drift in the transverse direction. Once both the electron density (n_{e}) and velocity (v) are known, the transverse electron current (J) can be calculated as the following:

$$J(t) = -\int ev(t,t')\,\mathrm{d}n_{\mathrm{e}}(t'). \quad (11)$$

The E_{rad} is the electric field is being radiated by the first time derivative of the electron current ($\mathrm{d}J/\mathrm{d}t$). Therefore, it is proportional with the THz field in the low frequency regime. In our research the cut-off frequency of the THz spectrum is chosen to be 8.8 THz, which is a commercially available THz low pass filter. More broadband THz low pass filters are also available commercially, but in that case a portion of the fundamental pulse may also pass through, which would make it difficult to characterize the THz pulse itself. Furthermore, previous studies [32, 33] found that the photocurrent model are more accurately describes the THz pulse generation at the low frequency regime (<10 THz).

3. Theoretical arrangement

In our numerical model, the so-called common path scheme was considered for the combination of the fundamental and its second harmonic pulses, as shown in figure 2. The earlier mentioned phase matching condition (type I) for the SHG, means that the fundamental pulse is ordinary (o) polarized, while its second harmonic is extraordinary (eo) polarized. These perpendicular polarizations are unsuitable for efficient THz pulse generation since the phenomenon is most efficient with parallel polarizations [34]. There are two possible solutions to

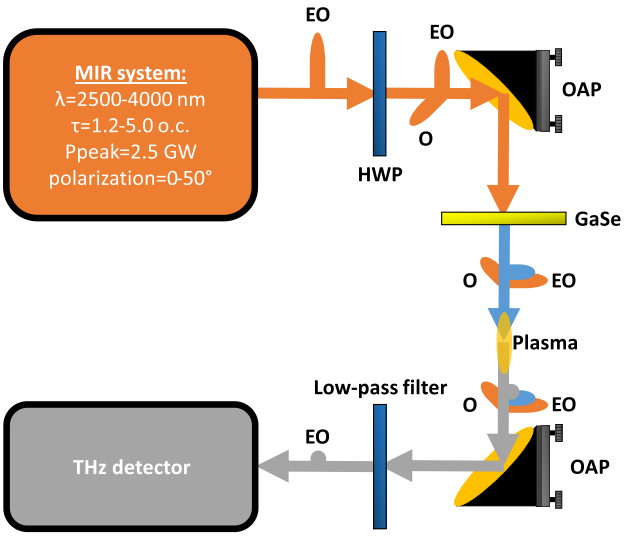

Figure 2. Schematic figure of the THz pulse generation with few-cycle, MIR laser pulses. The orange, blue and grey colors indicate the fundamental, the second harmonic and the THz pulses, respectively. HWP—half-wave plate; OAP—off-axis parabolic mirror; O—ordinary polarized pulse; EO—extraordinary polarized pulse.

overcome this inconvenience and optimize the polarizations. The most straightforward approach would be using dual wave-plates; however, they are not widely available in the MIR spectral region to the best of the authors' knowledge. The less straightforward solution is detuning the phase matching condition during the SHG in the nonlinear crystal to achieve partially overlapping polarizations [35]. In this approach, a minor portion of the fundamental pulse is ordinary (o) polarized, while the major portion is extraordinary (eo) polarized. The former generates the second harmonic pulse in the nonlinear crystal, while the latter generates the THz pulse in the focus accompanied with the SH pulse, which is also extraordinary (eo) polarized. Commercially available GaSe nonlinear crystals come with different thicknesses; however, we selected the thinnest commercially available crystal (10 μm) for our simulations as a source of broadband SH pulse. Thicker crystals (30, 100 μm and etc) are also commercially available, but they are not suitable for broadband SH pulse generation. In our numerical model we considered this latter solution.

To avoid. any absorption during propagation, the whole beam path was considered to be in dry nitrogen at atmospheric pressure, with dispersion taken into account based on the generalized Sellmeier equation [36].

The pulse peak power (2.5 GW) was kept at a constant level. The investigated spectrum ranged from 2500 to 4000 nm, which is a typical value for laser systems operating in the MIR spectral regime, such as the MIR laser system at ELI-ALPS Research Institute [37], and the other parameters of the simulation also mimic this system. The full width at half maximum beam diameter was 27.5 μm in the focus and 1.0 mm at the GaSe crystal. Both the temporal and spatial shapes of the pulse were chosen to be Gaussian. The calculated intensity and peak electric field are 1.5×10^{15} W m^{-2} and 7.5×10^{5} kV m^{-1} at the GaSe, respectively.

4. THz pulse generation

One of the aims of our simulation is to reveal the efficiency of THz pulse generation with few-cycle, MIR laser pulses as a function of the pulse duration of the driving laser pulse. Here, the pulse duration range is varied from 1.2 to 5.0 optical cycles. Our work indicates that both the Kerr-effect induced positive and the plasma-induced negative refractive index changes are orders of magnitude smaller than the refractive index of nitrogen at the power and intensities investigated here. Therefore, Kerr-effect induced focusing and plasma induced de-focusing are neglected in our numerical simulations. Intensity clamping is also neglected since it is an equilibrium between Kerr-effect induced focusing and plasma induced defocusing.

First, we examined how the variation of the duration and polarization angle of the fundamental pulse affect THz pulse generation. The examined polarization angles of the pulse changed from 0° to 50°, where 0° is the purely extraordinary (eo) polarization and 90° is the purely ordinary (o) polarization.

4.1. THz pulse generation with a fundamental pulse at 3200 nm carrier wavelength

Next, we investigated THz pulse generation at 3200 nm carrier wavelength of the driving laser pulse, which is a typical value for laser systems operating in the MIR spectral regime. Note that one optical cycle corresponds to 10.7 fs at this carrier wavelength. The results are shown in figure 3 in case of $\pm\pi/2$ rad relative phase between the fundamental and its SH pulses. For the $+\pi/2$ rad relative phase (see figure 3(a)), there are two regions, where THz pulses can be efficiently generated. The first is the two-color approach, where the two-color scheme is more effective. This can be seen in the bottom middle of figure 3(a) (highlighted with a solid white line). In this case, the maximum THz electric field is 11.0 kV m^{-1} at 5.0 optical cycle and 25° polarization angle. Interestingly, the calculation shows that there is a second region where THz pulse generation is just as efficient as in the two-color scheme. Here we employ a single color, i.e. only the fundamental laser pulse without SH pulse. This can be seen in the top left of figure 3(a) (highlighted with a dashed white line). In this case, the maximum THz electric field is 7.9 kV m^{-1} at 1.2 optical cycles and 0° polarization angle. As a reminder, the 0° polarization angle indicates that the fundamental pulse polarization is purely extraordinary, hence no SHG occurs in the GaSe crystal. In this scheme we can eliminate the nonlinear crystal. By this we can terminate reflection loss and also avoid the negative effect of dispersion on THz pulse generation, leading to further improvement in efficiency. The shift between the regions is continuous and it appears around 1.7 optical cycles (18.1 fs).

For the $-\pi/2$ rad relative phase (see figure 3(b)), there are also two regions for efficient THz pulse generation. As discussed above, the two-color approach can be seen in the

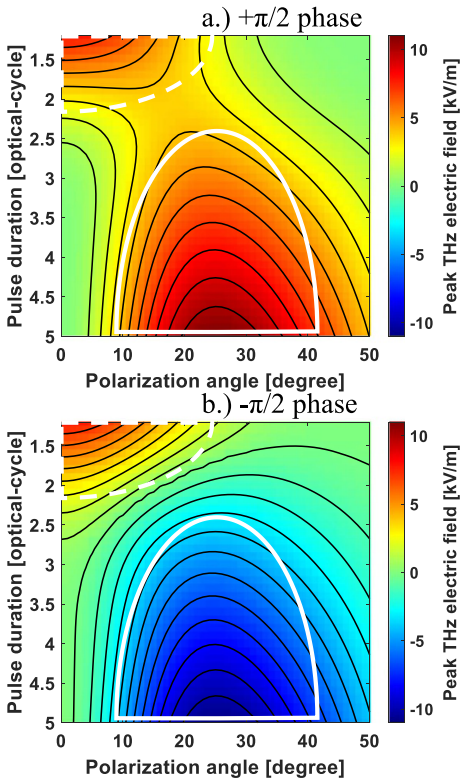

Figure 3. The THz pulse peak power as a function of the pulse duration and the polarization angle in case of (a) $+\pi/2$ rad and (b) $-\pi/2$ rad relative phase. The central wavelength of the driving laser pulse is 3200 nm.

bottom middle of figure 3(b) (highlighted with a solid white line). In this case, the absolute maximum, which is technically a minimum, THz electric field is -11.0 kV m^{-1} at 5.0 optical cycles and 25° polarization angle. As one can see, the sign of the THz electric field is inverted, when the sign of the relative phase is inverted. The single-color approach can be seen in the top left of figure 3(b) (highlighted with a dashed white line). In this case, the maximum THz electric field is 7.9 kV m^{-1} at 1.2 optical cycles and 0° polarization angle. As one can see, the sign of the THz electric field is not inverted, since the single-color scheme is independent of the second harmonic pulse. The shift between the regions is not continuous, and it occurs around 2.1 optical cycles (22.4 fs). In the case of $+\pi/2$ rad relative phase, both the single-color and two-color schemes generate THz pulses with a positive sign. However, in the case of $-\pi/2$ rad relative phase, the single-color scheme generates THz pulses with a positive sign, while the two-color scheme generates THz pulses with a negative sign. Because of this, in the former case the shift is continuous, while in the latter case it is not.

There is also a third, transition region between the single- and two-color schemes. The first is the already discussed single-color scheme, where single-color THz pulse generation becomes dominant. This region starts at 1.7 optical cycles (18.1 fs) and below. The second is the already presented two-color scheme, where two-color THz pulse generation is more efficient. Furthermore, THz pulse generation is not sensitive to the sign of the relative phase. The two-color scheme with $-\pi/2$ rad and $+\pi/2$ rad relative phase generates THz pulses with similar absolute peak powers but with an inverted sign. This starts approximately around 3.2 optical cycles (34.1 fs) and above. The third, transitional region is between the single-color and two-color regions, where two-color THz pulse generation is more efficient, but THz pulse generation is sensitive to the sign of the relative phase. The two-color scheme with $-\pi/2$ rad and $+\pi/2$ rad relative phase generates THz pulses with different absolute peak powers.

To better understand the transition between the single-color and two-color schemes, we explored the temporal evolution of the process through the steps of the numerical simulations. In this more detailed investigation, we selected a simulation where the central wavelength is 3200 nm and the pulse duration corresponds to 2.0 optical cycles (21.3 fs). The results are shown in figure 4. The blue lines indicate the single-color scheme at 0° polarization angle. The orange lines indicate the two-color scheme at 25° polarization angle in case of $+\pi/2$ rad relative phase, hereinafter positive two-color. The red lines indicate the two-color scheme at 25° polarization angle in case $-\pi/2$ rad relative phase, hereinafter negative two-color.

The temporal shapes of the external electric field in each case are shown in figure 4(a). It is a little more intense in case of the single-color scheme, than in both two-color schemes. This is due to the reduced losses (reflection and nonlinear conversion) of the fundamental pulse. The tail of the external electric fields in both two-color schemes are more asymmetric compared to the single-color scheme due to the presence of their associated SH pulse. The orientation of this asymmetry depends on the relative phase between the fundamental and its SH pulse.

The temporal evolution of electron density in each scenario is shown in figure 4(b). In case of the single-color scheme, it is 0.45%, while the electron densities of the positive and negative two-color schemes are only 0.16% and 0.15%, respectively. These values make up approximately one third of the single-color scheme, which is a consequence of the slightly less intense electric field. Please note that the ionization rate is an exponential function of the external electric field, hence a minor change in the external electric field could induces a major change in the electron density. In every case, ionization occurs in three significant steps. In case of the single-color and the positive two-color schemes, the second step is the most prominent, while in case of the negative two-color scheme, the first step is the most prominent, as it can be seen in figure 4(b).

The temporal evolution of the electron current in each case is shown in figure 4(c). In case of the single-color and positive two-color schemes, strong, positive currents build up because of the dominant second step during ionization, which overlaps temporally with the maximum of the external electric field. As a result, the first two steps of the electron current have different intensities and signs, which eventually leads to the development of a strong positive electron current. The permanent levels of the electron currents are similar, despite originate from different external electric fields. The external electric field is more intense and less asymmetric in case of the

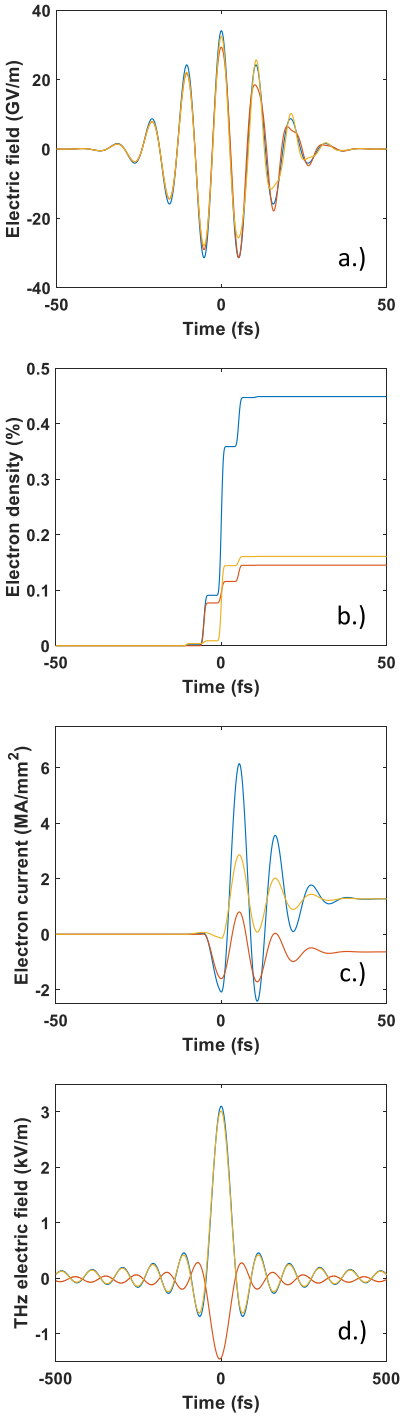

Figure 4. Temporal shapes of (a) the external electric field, (b) the electron density, (c) the electron current and (d) the THz electric field. The blue lines indicate the single-color scheme at 0° polarization angle. The orange and red lines indicate the positive and negative two-color schemes at 25° polarization angle, respectively. The central wavelength is 3200 nm and the pulse duration is 2.0 optical cycles (21.3 fs) in each case.

single-color scheme, while it is less intense, but more asymmetric in case of the positive two-color scheme. These results indicate that both properties play important roles in THz pulse

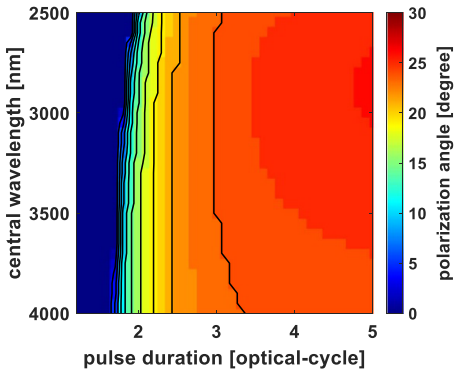

Figure 5. The optimal polarization angle of the fundamental pulse as a function of duration and the central wavelength in case of single-color versus positive two-color scheme. The corresponding THz electric field is shown in figure 6(a).

generation. In case of the negative two-color scheme, a weak negative current builds up due to the dominant first step during the ionization. The second step during ionization is less dominant, but it overlaps temporally with the maximum of the external electric field. The first two steps of electron current formation have similar intensities, but different signs, which means that they almost extinguish each other and develop a weak electron current in the end.

The THz electric fields of each case are shown in figure 4(d). In the single-color and the positive two-color schemes, a strong positive THz electric field builds up from the strong, positive electron currents. Since the electron currents are similar, the THz electric fields built up from them are also similar in these two cases. In the negative two-color scheme, a weak negative THz electric field builds up from the weak, negative electron current.

In conclusion, the most important parameters of the external electric field are intensity and asymmetry during the THz pulse generation. The generation of similar THz pulses is possible with different external electric fields. As far as intensity is concerned, the single-color scheme is preferred due to the fewer losses involved (reflection and nonlinear conversion). In terms of asymmetry, it is more advantageous to use the two-color schemes. However, the asymmetry increases with decreasing pulse duration in every scheme and as a result, in the case of few-cycle pulses, the single-color scheme will be more efficient as presented earlier.

4.2. THz pulse generation at different carrier wavelengths of the fundamental pulse

We investigated THz pulse generation from 2500 nm (one optical cycle is 8.3 fs) to 4000 nm (one optical cycle is 13.3 fs) carrier wavelength of the driving laser pulse, which is a typical value for laser systems operating in the MIR spectral regime. These results allow researchers to explore the effects of the central wavelength and the pulse duration of the driving pulse on THz pulse generation under realistic conditions. The results are shown in figures 5 and 6.

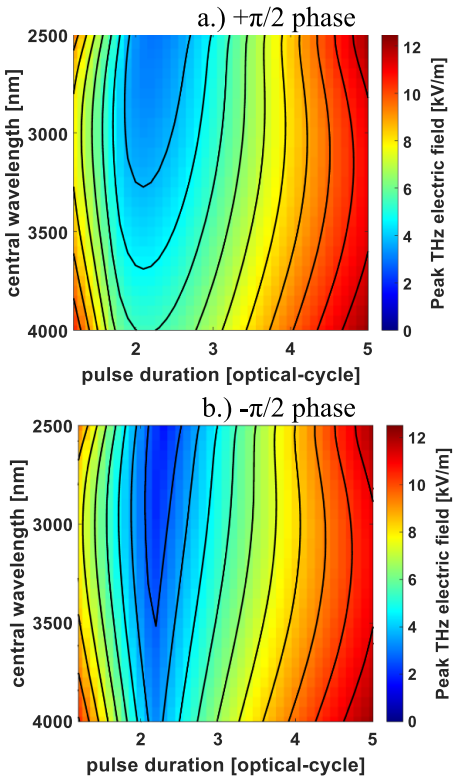

Figure 6. The optimal THz electric field of the fundamental pulse as a function of duration and the central wavelength in case of (a) single-color versus positive two-color scheme and (b) single-color versus negative two-color scheme.

The optimal polarization angle for single-color vs positive two-color schemes is shown in figure 5. When the optimal polarization angle equals 0°, the single-color scheme is more efficient than the positive two-color scheme. As a reminder, 0° polarization angle means that the fundamental pulse polarization is purely extraordinary, hence no SHG occurs in the GaSe nonlinear crystal. The shift between the two schemes that is the upper boundary of the single-color approach, is around 1.9 optical cycles (15.9 fs) and 1.6 optical cycles (21.3 fs) in case of 2500 and 4000 nm central wavelengths, respectively. As shown in figure 5, the boundary of the single-color approach decreases with increasing central wavelength.

The optimal THz electric field is shown in figure 6 for the single-color versus positive two-color schemes (figure 6(a)) and for the single-color versus negative two-color schemes (figure 6(b)). The lower boundary of the conventional region is determined by comparing the positive and negative two-color schemes. When the difference between the two schemes is less than 1%, then one can speak of the two-color approach. The lower boundaries of the two-color approach are around 3.2 optical cycles (26.7 fs) and 3.5 optical cycles (46.7 fs) in case of 2500 and 4000 nm central wavelengths, respectively. The boundary of the two-color approach increases with increasing central wavelength.

In conclusion, the most important result is that the upper limit (expressed in optical cycles) of the single-color approach increases, while the lower limit of the two-color approach decreases with increasing carrier wavelength. The former effect is likely to be related to the improving condition of the SHG. As the carrier wavelength increases, the efficiency of the SHG increases too, and the temporal overlap between the two-color pulses decreases. Both phenomena have a positive effect on THz pulse generation, which makes it understandable, why the increasing carrier wavelength makes it more difficult to reach and study the single-color approach. The latter effect is likely to be related to the increasing ponderomotive potential, which increases with the carrier wavelength. This explains why it is easier to reach and study the transient region.

5. The relative phase and the CEP effect on the THz pulse generation

Another important question is how the relative phase and the CEP impacts the THz pulse generation with few-cycle, MIR pules. The THz pulse generation in the function of the two phases shown in figure 7 in case of different pulse durations at a fixed polarization angle (20°). In the case of 3.0 optical cycle (32.1 fs) pulse duration (figure 7(a)), as one can see that the CEP (*X*-axis) does not have any visible effect on the THz pulse generation, however on the other hand the relative phase (*Y*-axis) has a significant effect on the THz pulse generation. In the case of 2.5 optical cycle (26.8 fs) pulse duration (figure 3(b)), as one can see the importance of the CEP increase, while the importance of the relative phase decrease as the durations of the pulse shortens. In the case of 2.0 optical cycle (21.4 fs) pulse durations (figure 3(c)), the former changes are even more visible and significant. These changes can be easily understood in the light of our previous results. As the duration of the pulse gets shorter the THz generations changes from the double-color scheme to the single-color scheme. This change is important for two reasons. First, as the duration of the pulse decrease the necessity of the SH pulse also decrease, which, for understandable reasons, also reduces the effect of the relative phase. Second, as the duration of the pulse increase the number of individual optical cycles increase and the difference between them decrease, which, for understandable reasons, reduces the impact of the CEP on THz pulse generation.

For convenience, only the CEP and the pulse durations effect are graphed on the THz pulse generation as shown in figure 8(a). As the pulse duration of the driving pulse reduces meanwhile the significance of the CEP becomes important. The sensitivity of the THz pulse generation is defined as follows:

$$S = \frac{\mathrm{THz}_{\max} - \mathrm{THz}_{\min}}{\mathrm{THz}_{\max}}. \tag{12}$$

The value of the sensitivity varies between 0 and 2. The 0 corresponds to a case when the THz generation is insensitive to the investigated parameter. In this case, the $\mathrm{THz}_{\max}$ and the $\mathrm{THz}_{\min}$, have the same sign and value. On the other hand, 2 corresponds to maximum sensitivity of the THz generation to the investigated parameter. In this case, the $\mathrm{THz}_{\max}$ and

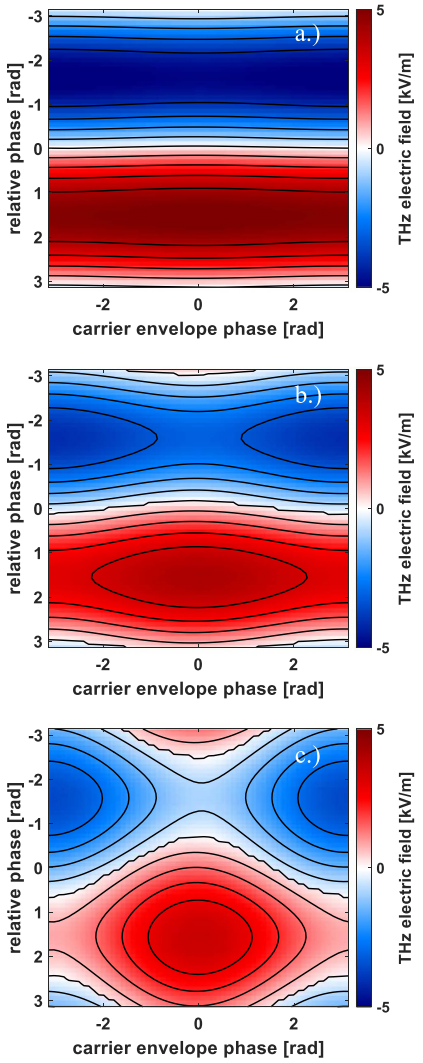

Figure 7. The peak electric field of the THz pulse in the function of the carrier to envelope and relative phase in case of (a) 3.0 cycle (32.1 fs), (b) 2.5 cycle (26.8 fs) and (c) 2.0 cycle (21.4 fs) pulse duration. The central wavelength of the driving laser pulse is 3200 m and the polarizations angle is 20°.

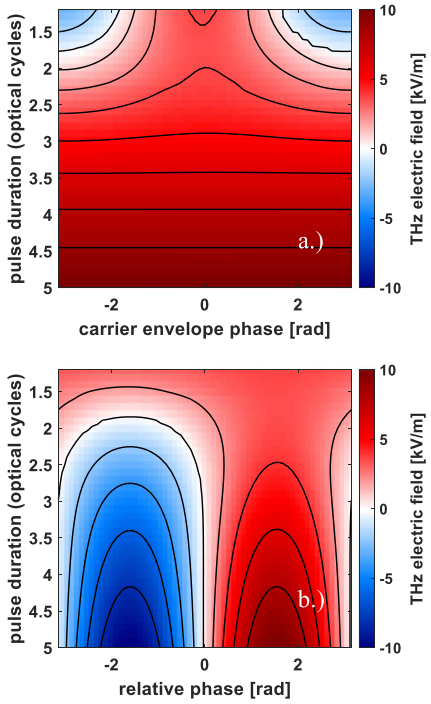

Figure 8. The peak electric field of the THz pulse in the function of the pulse duration and (a) the CEP and (b) the relative phase. The central wavelength of the driving laser pulse is 3200 nm and the polarization's angle is 20°.

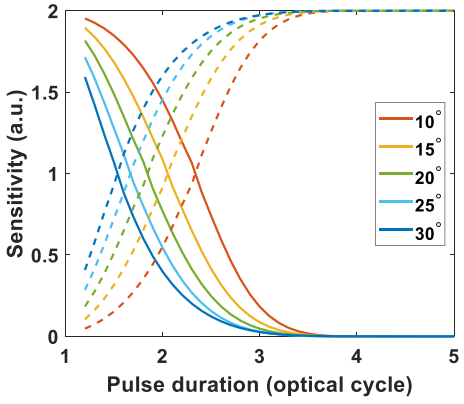

Figure 9. The sensitivity of the CEP (solid line) and the relative phase (dashed line) in the function of the pulse duration in case of different polarization angles indicated by different colors.

the THz_{min}, have the opposite sign and the same value. In all other cases, the value of sensitivity is between 0 and 2. The sensitivity of the carrier to envelope phase are 7.13×10^{-6}, 4.52×10^{-4}, 2.01×10^{-2} and 7.68×10^{-1} at 5.0, 4.0, 3.0 and 2.0 optical cycles, respectively.

The relative phase and the pulse duration also have an important contribution to the THz pulse generation as shown in figure 8(b). As the pulse duration reduces the influence of the of the relative phase decreases for THz pulse generation. The sensitivity of the relative phase are 2.00, 2.00, 1.95 and 1.23 at 5.0, 4.0, 3.0 and 2.0 optical cycles, respectively.

The sensitivity of the CEP (straight line) and the relative phase (dashed line) in the function of the pulse duration in case of different polarization angles indicated by different colors, shown in figure 9. The switching point is defined, where the two sensitivities are equal, and it clearly depends on the polarization angle. The switching point is below 2.3, 2.1, 1.9, 1.7 and 1.6 optical cycles at 10°, 15°, 20°, 25° and 30° polarization angle, respectively. We think that the reason behind this phenomenon is the SHG itself. As the polarization angle decrease, the generation efficiency of the SHG also decrease, which reduces the relative phase importance, which increases the position of the switching point. Based on these results, it becomes possible to develop a CEP measurement technique.

For few-cycle pulses, the measurement of the pulse duration and the control of the CEP is paramount interest.

6. Summary

We have carefully investigated THz pulse generation as a function of the pulse duration and polarization angle of the driving pulse at 3200 nm carrier wavelength. Three different regions have been identified, where the optimal laser pulse parameters are fundamentally different for efficient THz pulse generation. Around 3.2 optical cycles (34.1 fs) and above, the two-color approach is dominant. However, around 1.7 optical cycles (18.1 fs) and below, the single-color approach prevails. There is also a transitional region between the single-color and the two-color schemes. In this region the two-color approach is still dominant, but the sign of the relative phase becomes important. In addition, we have found that the lower boundary of the two-color scheme increases, while the upper boundary of the single-color scheme decreases, when one increases the central wavelength of the driving pulse.

We have also examined the CEP and the relative phase effect on the THz pulse generation as a function of the pulse duration and the polarization angle at 3200 nm central wavelength. We have found that the sensitivity of the CEP becomes important, while the sensitivity of the relative phase becomes less crucial with decreasing pulse duration. Interestingly, the switching point is somewhat sensitive to the polarization angle. Specifically, when the polarization angle decrease, the switching point shifts to longer values of pulse durations.

The numerical results presented in this study will provide important insights for future experiments where the aim is to generate more intense THz pulses with few-cycle, MIR laser pulses. The single-color scheme has been used previously to generate THz pulses; but the two-color scheme has proven to be more efficient in the past. The results reported in this article and as few-cycle, MIR laser pulses become widely available will provide new opportunities in THz science. In addition, the THz pulses might provide diagnostic information about the CEP, an important parameter for the broader laser community for efficient control of laser parameters.

Data availability statement

The data that support the findings of this study are available upon reasonable request from the authors.

Acknowledgment

The ELI-ALPS Project (GINOP-2.3.6-15-2015-00001) is supported by the European Union and co-financed by the European Regional Development Fund.

ORCID iDs

Roland Flender https://orcid.org/0000-0001-6970-0716
Adam Borzsonyi https://orcid.org/0000-0001-5287-5456
Viktor Chikan https://orcid.org/0000-0002-4157-3556

References

[1] Mayer B W 2014 *Opt. Express* **22** 20798
[2] Baudisch M 2015 *J. Opt.* **17** 094002
[3] Baudisch M 2016 *Opt. Lett.* **41** 3583
[4] Elu U 2017 *Optica* **4** 1024
[5] Thire N 2017 *Opt. Express* **25** 1505
[6] Thire N 2018 *Opt. Express* **26** 26907
[7] Popmintchev T 2012 *Science* **336** 1287
[8] Clerici M 2013 *Phys. Rev. Lett.* **110** 253901
[9] Nguyen A 2017 *Opt. Express* **25** 4720
[10] Nguyen A 2018 *Phys. Rev.* A **97** 063839
[11] Fedorov V Y 2018 *Phys. Rev.* A **97** 063842
[12] Fedorov V Y 2018 *Opt. Express* **26** 31150
[13] Nguyen A 2019 *Opt. Lett.* **44** 1488
[14] Koulouklidis A D 2020 *Nat. Commun.* **11** 292
[15] Flender R 2020 *J. Opt. Soc. Am.* B **37** 1838
[16] Reduzzi M 2015 *J. Electron. Spectrosc. Relat. Phenom.* **204** 257
[17] Jang D 2019 *Optica* **6** 1338
[18] Kim K Y 2012 *IEEE J. Quantum. Electron.* **48** 797
[19] Kim K Y 2007 *Opt. Express* **15** 4577
[20] Hemmer M 2013 *Opt. Express* **21** 28095
[21] Shumakova V 2016 *Nat. Commun.* **7** 12877
[22] Marcinkeviciute A 2017 *J. Opt.* **19** 105505
[23] Lu F 2018 *Opt. Lett.* **43** 2720
[24] Kurucz M 2020 *Opt. Commun.* **472** 126035
[25] Flender R 2021 *J. Opt.* **23** 065501
[26] Boyd R W 2008 *Nonlinear Optics* (New York: Academic) pp 69–134
[27] Kato K 2013 *Appl. Opt.* **52** 2325–8
[28] Allakhverdiev K R 2009 *Laser Phys.* **19** 1092–104
[29] Kogelnik H 1966 Laser Beams and Resonators *Appl. Opt.* **5** 1550–67
[30] Ammosov M V 1986 *J. Exp. Theor. Phys.* **64** 1191–4
[31] Rodriguez G 2001 *IEEE J. Sel. Top. Quantum Electron.* **7** 579–1
[32] Aandreeva V 2016 *Phys. Rev. Lett.* **116** 063902
[33] Wang H 2018 *Phys. Rev.* A **98** 013857
[34] Xie X 2006 *Phys. Rev. Lett.* **96** 075005
[35] Kress M 2004 *Opt. Lett.* **29** 1120–2
[36] Voronin A A 2017 *Sci. Rep.* **7** 46111
[37] (available at: https://eli-alps.hu)